Published in final edited form as:

Cancer Res. 2011 December 01; 71(23): 7301–7311. doi:10.1158/0008-5472.CAN-11-2381.

LPA receptor heterodimerizes with CD97 to amplify LPA initiated Rho-dependent signaling and invasion in prostate cancer cells

Yvona Ward[1], **Ross Lake**[1], **Juan Juan Yin**[1], **Christopher D. Heger**[2], **Mark Raffeld**[3], **Paul K. Goldsmith**[2], **Maria Merino**[4], **Kathleen Kelly**[1,+]

[1]Cell and Cancer Biology Branch, Center for Cancer Research, NCI, Building 37, Room 1068, Bethesda, MD 20892

[2]Antibody and Protein Purification Unit, Center for Cancer Research, NCI, Building 37, Room 6134, Bethesda, MD 20892

[3]Laboratory of Pathology, Center for Cancer Research, NCI, Building 10, Room 2N110, Bethesda, MD 20892

[4]Laboratory of Pathology, Center for Cancer Research, NCI, Building 10, Room 2N212, Bethesda, MD 20892

Abstract

CD97, an adhesion-linked G-protein coupled receptor (GPCR), is induced in multiple epithelial cancer lineages. We address here the signaling properties and the functional significance of CD97 expression in prostate cancer. Our findings show that CD97 signals through Gα12/13 to increase RHO-GTP levels. CD97 functioned to mediate invasion in prostate cancer cells, at least in part by associating with lysophosphatidic acid receptor 1, (LPAR1), leading to enhanced LPA-dependent RHO and ERK activation. Consistent with its role in invasion, depletion of CD97 in PC3 cells resulted in decreased bone metastasis without effecting subcutaneous tumor growth. Furthermore, CD97 heterodimerized and functionally synergized with LPAR1, a GPCR implicated in cancer progression. We also found that CD97 and LPAR expression were significantly correlated in clinical prostate cancer specimens. Taken together, these findings support the investigation of CD97 as a potential therapeutic cancer target.

Keywords

CD97; LPA; RHO; prostate cancer; invasion

Introduction

Expression of the G-protein coupled receptor (GPCR) CD97 is induced in a variety of epithelial cancers. CD97 is normally expressed on cells of hematopoetic origin and smooth muscle but is expressed at very low levels or is absent in normal epithelial cells (1, 2). Carcinomas derived from various epithelial tissues consistently demonstrate increased CD97

[+]corresponding author: Kathleen Kelly, kellyka@mail.nih.gov, 301-435-4651.

expression compared to normal adjacent tissue and in some cases, the level of CD97 expression positively correlates to tumor grade and poor prognosis. CD97 induction has been described in thyroid (3), colorectal (4), gastric, pancreatic, esophageal (3), oral squamous cell (5), and prostate carcinomas (6). It has been unclear as to whether CD97 is a marker of epithelial transformation, or alternatively, might play a functional role. Of interest is the description of CD97 at the invasion front of carcinomas, hinting at a potential function in progressing cells (3). However, the existence of CD97-dependent signaling associated with tumors has not been established. Here we have investigated whether CD97 plays a functional signaling role in prostate cancer.

CD97 is a member of the adhesion-linked GPCRs, a family of membrane-bound proteins characterized by a large extracellular subunit containing one to a few adhesion motifs noncovalently associated with a conserved GPCR seven-transmembrane domain (TM7) (7). Most adhesion-linked GPCRs are translated as a single polypeptide that is proteolytically processed intracellularly to produce the two associated subunits. CD97 belongs to a subclass of adhesion GPCRs that contain variable numbers of EGF-like repeats in the extracellular adhesion domain (1). Although the adhesion GPCR family members are thought to have the dual potential of cellular adhesion and signaling, a mechanistic understanding of adhesion coupled signaling has not been established (2). Heterotrimeric $G\alpha_{12/13}$ dependent signaling has been shown for one family member, GPR56, but signaling has not as yet been linked to binding of the known ligand, Transglutaminase 2 (8, 9). In addition, two receptors, BAI1 and LTR, have known ligand-dependent functions which require the transmembrane regions, but it has not been established functionally whether heterotrimeric G-protein signaling is needed (10, 11). Specific CD97 isoforms have been shown to interact with integrins $\alpha5\beta1$ and $\alpha v\beta3$ (12), the cell surface complement regulatory protein CD55 (13), and the extracellular matrix component chondroitin sulfate (14), although ligand-dependent signaling has not been shown.

In the present study we demonstrate that CD97 complexes in cis with and positively regulates LPAR1, a cognate receptor for lysophosphatidic acid (LPA), resulting in increased LPA-dependent RHO signaling. LPA is a bioactive phospholipid that acts as a high affinity ligand for LPARs to mediate various cellular functions that contribute to transformation including proliferation, survival, cytoskeletal restructuring, and production of secreted factors such as cytokines and metalloproteases (15, 16). Bioactive LPA is produced in the extracellular matrix when complex lysopholipids, predominantly lysophosphatidylcholine, are hydrolyzed by the secreted enzyme, autotoxin (ATX). Elevated LPA production (17) and increased expression of cell surface LPARs (18, 19) have been reported for various human carcinomas, including prostate cancer. Using a transgenic mouse model, Liu et al. (20) demonstrated directly that ATX and LPARs 1, 2, and 3 contribute to the initiation and progression of breast cancer. We describe here in prostate cancer a functional association between CD97 and LPAR1 that modifies LPA-initiated signaling, a finding that lends mechanistic understanding to the potential importance of CD97 induction in carcinomas.

Materials and Methods

The following technical information is provided in the Supplementary Data: “Antibodies and Reagents,” ” Expression Constructs,” “Immunohistochemistry,” “SRE-luciferase reporter assay,” “Facs analysis and cell sorting,” “CD97 silencing,” and “In situ proximity ligation assay.”

Cell-culture

DU145, PC3, and LNCaP prostate cancer cells were obtained from ATCC. PC3 cells permanently expressing a luciferase reporter were generated and cultured as reported (21). All culture media and reagents were from Invitrogen.

Immunofluorescence and confocal microscopy

Staining and image acquisition by confocal microscopy were carried out as previously described (22). Mouse monoclonal antibodies directed against HA and vinculin were used at a 1:1000 dilution.

Preparation of cell blocks

Prostate cells were made into cell blocks using the fibrin clot method as described (23). Blocks were fixed in 10% formalin and paraffin embedded. Sections were prepared and stained using the immunohistochemistry procedure.

Immunoprecipitation and western blot analysis

Relative levels of myc-tagged CD97–3EGF and myc-tagged CD97β were determined by transfecting COS 7 cells with varying amounts of DNA using Lipofectamine Plus. Lysates were prepared and immunopreciptations and western blots were performed as described (24). Coimmunoprecipitation assays were performed as described (25). The amount of GTP bound RHOA was determined using the RHO activation assay kit (Upstate Cell Signaling Solutions).

In vitro invasion and migration

Invasion chambers were prepared as described previously (12) except that growth factor reduced matrigel (BD Bioscience) was used. DU145 cell invasion was performed as described (25). For Rho inhibition cells were resuspended in medium containing CT04 (2μg/ml). PC3 and LNCaP transmigration was set up as described above except that BSA was not added to the serum free media and cells were allowed to migrate for 24 hours. Migration was carried out the same way as in vitro invasion except that the membrane was coated with gelatin instead of matrigel.

PC3 metastasis assay

Experimental metastasis assays and bioluminescent imaging were done as described previously (21).

Results

CD97 expression is induced in prostate adenocarcinomas and is expressed in some prostate cancer cell lines.

Immunohistochemical analysis of a prostate cancer tissue array indicated that CD97 was expressed in the membrane and cytoplasm of adenocarcinoma cells while it was undetectable in normal adjacent prostate epithelium (Fig. 1A). For the majority of prostate cancer samples, the CD97 staining intensity was relatively uniform, while the percentage of positive cells varied (Table 1). Fifty-nine percent of the adenocarcinomas were positive for CD97 with the majority (44.1%) demonstrating positive CD97 staining in 50–80% of adenocarcinoma cells. In the prostate tissue array 68% of adenocarcinomas with Gleason score 6–7 and 53% of adenocarcinomas with Gleason score 8–10 were stained positively for CD97 expression. The specificity of the rabbit polyclonal anti-CD97 antibody used to stain the prostate tissue array was verified by staining paraffin embedded prostate epithelial cells with known CD97 expression patterns (Supplementary Fig. 1).

FACS analysis of various prostate cell lines stained for CD97 revealed differential cell surface expression. Non-transformed, primary prostate cells (RWpE-1) were negative, while we observed both positive (PC3 and DU145) and negative (22RV1 and LNCaP) prostate adenocarcinoma-derived cells lines (Fig. 1B). Western blot analysis produced similar results except that 22RV1 cells appeared to express very low levels of CD97 not detected by the FACS analysis (Fig. 1C). The expression patterns of CD97 in the prostate cancer tissue array and in different prostate cell lines confirm an earlier report that CD97 is induced in prostate adenocarcinomas (6).

Ectopic overexpression of CD97 stimulates $G\alpha_{12/13}$ dependent RHOA activation

Although CD97-mediated signaling has not yet been elucidated, the conserved GPCR transmembrane structure of CD97 suggests that its function is G-protein coupled. There are a number of examples of highly-expressed GPCRs that induce signal activation in a ligand-independent manner (26). Here we combined ectopic CD97 overexpression with assays for various signal transduction pathways. We observed CD97-dependent induction of activity for the transcriptional reporter SRE-luciferase, an indicator of RHOA activity that is commonly used to assay $G\alpha_{12/13}$ activation (27). Transient transfection of COS 7 cells with constitutively activated forms of RHOA and $G\alpha_{12}$ but not $G\alpha_q$ (Fig. 2A) resulted in significantly elevated levels of normalized SRE-dependent luciferase activity, verifying the expected specificity of the assay.

A variety of CD97 receptor configurations were assayed including 1) full-length CD97 containing either three or five EGF-like repeats, 2) the GPCR portion of CD97 (denoted CD97β), and 3) a GPCR-deficient control (denoted CD97-TM1) which consists of the extracellular region and only the first transmembrane segment. Full-length CD97 stimulated about a four-fold increase in activity, while GPCR-deficient CD97 was inactive. It is of interest that the CD97 GPCR β subunit alone stimulated a 50-fold increase in SRE-luciferase activity, suggesting higher constitutive activity of the β subunit in the absence of the interacting extracellular domain (note the scale difference between the left and right

panels of Fig. 2A). To normalize SRE activity relative to the level of CD97 GPCR subunit expression, the amount of DNA encoding C-terminal epitope-tagged full-length or β only CD97, was titrated in transfections and the transfected cells were subsequently assayed for protein amount and luciferase activity. A comparison of similar levels of GPCR subunit expression (Fig. 2C) showed a five-fold increase for full-length CD97 and a 19-fold increase for the β construct in SRE-luciferase activity.

To determine whether CD97-stimulated SRE activity was dependent upon $G\alpha_{12/13}$, an expression plasmid encoding the RGS domain (residues 1–246) of p115 Rho-GEF was co-transfected with CD97. As expected, RGS-p115 demonstrated $G\alpha_{12/13}$ specific inhibition but did not decrease downstream signals such as constitutively active RHOA-dependent SRE activity. As shown in Figure 2A, RGS-p115 almost entirely inhibited full-length CD97-dependent SRE activity and inhibited about 80% of CD97β-dependent SRE activity. To investigate whether SRE activation by CD97 was RHO-dependent, an expression construct for C3 exoenzyme, which specifically inhibits RHO as a result of ADP-ribosylation, was co-transfected with CD97 or control plasmids into COS 7 cells. The C3 exoenzyme blocked RHOA-dependent SRE activity, as expected. In addition, $G\alpha_{12}$-dependent SRE activity was substantially inhibited, indicating that the $G\alpha_{12}$-stimulated activity was predominantly through RHO activation. All CD97-stimulated SRE-luciferase activity was inhibited by C3 exoenzyme demonstrating strong RHO-dependence (Fig. 2B). No effect of C3 exoenzyme on cotransfected HSV-TK promoter driven Renilla expression was observed.

To further analyze the effects of sustained CD97 signaling, we generated clones of CHO cells expressing moderate levels of CD97β. These clones displayed a flattened morphology with pronounced stress fibers and uniformly distributed focal adhesions compared to clones expressing empty vector (Fig. 2D). Treatment of CHO cells expressing CD97β with a cell permeable specific inhibitor of RHO (CT04) caused a reduction in stress fibers and focal adhesions and resulted in complete reversion of the flattened phenotype back to that of cells expressing empty vector (Fig. 2D). Likewise, transient expression of wild type RHOA in CHO cells resulted in the same flattened morphology, which was readily reversed by treatment with CT04 (Fig. 2E), demonstrating that this cytoskeletal change is characteristic of RHO activation in CHO cells.

Depletion of CD97 in DU145 leads to inhibition of RHO-dependent, LPA-initiated, downstream signaling and invasion

To investigate potential physiological functions associated with CD97 expression in prostate cancer, endogenous CD97 expression was depleted using ectopic shRNA in two prostate cancer cell lines, DU145 and PC3 (Figures 3A and Supplementary 3). Depletion of CD97 expression in DU145 cells resulted in substantial inhibition of RHOA-GTP levels (Fig. 3A), suggesting that CD97 influences constitutive signaling in DU145. In addition, directed cell migration (Supplementary Fig. 2) and invasion (Fig. 3B) stimulated by 10% fetal bovine serum were significantly decreased following CD97 knockdown. Inhibition of RHO activity and in vitro invasion were readily rescued by introduction of an shRNA insensitive mutant of CD97–3EGF (Fig. 3A and B) indicating that the observed effects were specific to CD97. Treatment of DU145 cells with CT04 suppressed invasion of both control and CD97-

depleted cells to the same baseline level, showing that the majority of CD97-dependent migration was RHOA-dependent (Fig. 3B). We also investigated the impact of CD97 depletion on potential $G\alpha_{12/13}$ downstream mediators that are known to play a role in cellular migration and invasion. Figure 3C shows that CD97 depletion led to decreased phospho-ERK and phospho-AKT levels that were restored to parental DU145 levels by CD97 re-expression. We did not observe an effect on cell growth in vitro.

Because CD97-depleted DU145 cells exhibited reduced invasion to fetal bovine serum in vitro, we investigated chemoattractant constituents of serum and their ability to stimulate CD97-dependent cell invasion. A major chemoattractant found in serum is lysophosphatidic acid (LPA). A dominant pathway downstream of LPA receptors (LPAR) is $G\alpha_{12/13}$-mediated activation of RHOA and ERK (28). Another component of serum that is known to stimulate prostate cell invasion is hepatocyte growth factor (HGF), a ligand for the tyrosine kinase receptor, MET.HGF signals through PI3K and PAK4 (29) as well as ERK and AKT (30, 31).

LPA initiated signaling was assayed in parental and CD97-depleted cells, and we observed reductions in RHOA-GTP, phospho-ERK and phospho-AKT levels, similar to the pattern previously seen in CD97-depleted cells grown in serum-containing medium. By contrast, for HGF-stimulated cells, CD97 depletion reduced the relatively weak RHO-GTP signal but had minimal effects upon phospho-ERK and phospho-AKT levels (Fig. 3D) suggesting that CD97 does not have an impact on the dominant signaling downstream of HGF. Consistent with the signaling data, CD97 depletion had the most dramatic inhibitory effect upon RHO-dependent LPA-stimulated invasion (Fig. 3E). By contrast, for PI3K-dependent HGF-stimulated chemotaxis, CD97 levels had a minimal effect. Our results indicate that the consequences of depleting CD97 in DU145 cells were strongest for LPA-stimulated RHO-dependent invasion and signaling, although there was also a weak, mostly RHO-dependent effect on HGF initiated invasion and signaling. This weak effect may be a result of the cross-talk between the LPA and c-MET receptors or their downstream components (32, 33).

CD97 depletion in PC3 cells reduces experimental bone metastasis but not subcutaneous growth.

To address the role of CD97 in tumorigenesis and experimental metastasis, we used the PC3 prostate cancer cell line transfected with a luciferase expression construct (PC3-luc).Figure 4A shows that shRNA-mediated knockdown of CD97 in PC3 cells resulted in suppression of GTP-bound RHO and ERK activity, consistent with our findings for DU145 cells. However, phosphorylation of AKT was not affected by CD97 expression in PC3 cells. Similarly to DU145, invasion of PC3 cells to LPA was significantly reduced following CD97 knockdown or addition of CT04, indicating that the invasion was predominantly CD97 and RHO-dependent (Fig.4B). There was no apparent effect of CD97 depletion upon cell growth in vitro.

The impact of suppressing CD97 expression in PC3 cells was determined in vivo by subcutaneous growth and experimental metastasis. Following inoculation of cells into the flanks of immunocompromised mice, subcutaneous growth of PC3-luc cells was first observed after 7 days and was monitored through day 27. Loss of CD97 did not appear to inhibit the subcutaneous growth of PC3-luc cells. For the CD97 deficient population, 14 of

14 inoculations resulted in tumors with an average tumor volume of 118 ± 70 mm^3 at day 27. For the control population, 12 of 14 inoculations resulted in tumors with an average tumor volume of 92 ± 71 mm^3. Metastases of PC3-luc cells were analyzed after inoculation via the left cardiac ventricle (Table 2). Mice were imaged for bioluminescence after inoculation and then once per week starting at week 3 until morbidity. PC3-luciferase cell populations displayed tropism to bone including jaw, long bones, and vertebral bodies, and the distribution of metastatic sites was approximately the same in the experimental and control groups. Figure 4C shows representative bioluminescence and histological images for each of the metastatic sites. Table 2 shows the relative degree of metastasis in mice injected with parental PC3 cells and CD97 depleted cells. Of the mice injected with parental PC3 cells, approximately 93% (14/15) developed metastatic lesions while 55% (12/22) of mice inoculated with CD97 depleted PC3 cells developed bone metastasis. In addition, metastasis formation was significantly decreased from 2.07 tumors per mouse injected with the parental population to 0.77 tumors per mouse in those injected with the CD97 knockdown population. There was not a statistically significant difference between the growth rates of established tumors as determined by their mean bioluminescence over time. Metastases were confirmed by necropsy, and portions of lesions were subjected to histological analysis. No histological differences between CD97 deficient and parental populations were apparent (Fig 4C). Taken together, this data suggests that CD97 expression has a significant effect upon the ability of PC3 cells to initiate metastasis, consistent with effects upon migration, invasion, and/or colonization.

CD97 heterodimerizes with LPA receptor 1 resulting in enhanced invasion

Mechanistic studies were pursued to investigate the significant effect of CD97 depletion on LPA-initiated invasion and signaling. There is increasing evidence that G-protein coupled receptors can exist as selective heterodimers with specific ligand responses. We hypothesized that CD97 regulates RHO activity in prostate cancer cells at least in part by interacting with LPA receptors. LPAR1, which is expressed in PC3 and DU145 but not LNCaP, has been linked to LPA-initiated migration (18, 19). Techniques to assay an LPAR1-CD97 interaction are limited by a lack of sufficiently sensitive precipitating antibodies for endogenous levels of LPAR1 protein. Therefore, we generated constructs coding for tagged proteins to first analyze the CD97-LPAR1 interaction (Fig.5A). CHO cells were transiently transfected with HA-tagged LPAR1 and myc-tagged CD97–3EGF, and antibodies directed to either myc or to HA coimmunoprecipitated the other GPCR, indicating an interaction between LPAR1 and CD97 (Figure 5B).

We used the same strategy to look at LPAR1-CD97 heterodimer formation in LNCaP prostate cancer cells that are known to lack LPAR1 (18) and CD97 (Fig. 1B and C). LPAR1-HA, CXCR4-HA, and CD97-myc were permanently transfected into LNCaP cells in the appropriate combinations and assayed for cell surface expression (Supplementary Figure 3). In coimmunoprecipitation studies, an LPAR1-CD97 interaction was readily detectable (Fig. 5C) while CXCR4 coimmunoprecipitated far less CD97. To independently confirm LPAR1-CD97 interactions, we used the in situ proximity ligation assay (DuoLink) to detect heterodimer formation in permanently-transfected LNCaP cells (34). The red dots on the cell membranes shown in Figure 5D indicate the localization of interacting proteins confirming

that interacting LPAR1 and CD97 are in the same cell. Quantifications of the average signals or heterodimers for each cell line (Fig. 5E) demonstrated significant interaction between LPAR1 and CD97, whereas the degree of interaction between CXCR4 and CD97 was substantially lower. To verify that the introduced HA-tagged LPAR1 would interact with endogenous CD97, we used a lentiviral infection system to express HA-tagged LPAR1 in parental DU145 cells and in DU145 cells with depleted CD97. HA-tagged LPAR1 was expressed on 68% of the permanently transduced parental cells and on 65% of the CD97-depleted cells. Using the DuoLink assay we observed that endogenous CD97 heterodimerizes with introduced LPAR1 in DU145 cells and that the LPAR1-CD97 interaction is lost upon CD97 depletion (Fig. 5F).

To determine if formation of CD97-LPAR1 heterodimers enhances LPA- stimulated invasion in LNCaP cells, we subjected cells expressing each receptor alone or both LPAR1 and CD97 or CXCR4 and CD97 to invasion through a thin layer of matrigel. The chemoattractants LPA and SDF-1 were used for LPAR1 and CXCR4, respectively. Figure 5G shows that LPAR1 expression was sufficient to allow LPA-initiated migration, and that coexpression of CD97 and LPAR1 in LNCaP cells resulted in enhanced RHO-dependent invasion relative to LPAR1 alone. By contrast to LPA-stimulated migration, SDF-1 stimulated a weak migratory response in CXCR4 expressing cells that was not improved by CD97 coexpression (Fig. 5H). We conclude from our findings that CD97 and LPAR1 form heterodimers resulting in enhanced cell invasion in response to LPA stimulation.

CD97 expression positively correlates with LPAR1 in a prostate tissue array

For LPAR1-CD97 heterodimerization to be relevant for clinical prostate cancer, both receptors would be expected to co-occur in individual specimens of adenocarcinomas. The frequency of LPAR1 expression in prostate adenocarcinomas was investigated in tissue array samples that had been previously characterized for CD97 staining. Histological staining demonstrated that LPAR1 was expressed in a majority of epithelial cells in most samples of normal prostate (Supplementary Fig.4) unlike CD97 (Fig 1A). In addition, about 80% of adenocarcinomas demonstrated staining for LPAR1 with a shift toward more intense staining relative to normal prostate (Supplementary Figure 4 and Table 1). Interestingly, statistical analysis (Fisher's Exact Test) revealed a significant association between the presence of CD97 and LPAR1 expression ($P \leq 0.01$) in adenocarcinomas.

Discussion

The abnormal expression of CD97 in carcinomas has been described for various tissue origins. Here we show CD97 expression in clinical samples of prostate adenocarcinoma occurred at a high frequency (60%) across Gleason grades, while there was no detectable expression in normal prostate. An earlier study using a different antibody reported enhanced CD97 expression in prostatic intraepithelial neoplasia and localized prostate cancer relative to low levels of expression in normals (6). Taken together, these data suggest that CD97 induction occurs early in prostate cancer progression. The potential significance of induced CD97 expression in prostate adenocarcinoma was investigated by analyzing the signaling

properties of CD97 and the functional contribution of CD97 to prostate cancer invasion and experimental metastasis.

We show here that ectopic CD97 induces $G\alpha_{12/13}$-dependent RHOA activation, demonstrating intact heterotrimeric G-protein dependent signaling for the CD97β subunit. Depletion of endogenous CD97 in DU145 and PC3 cell lines inhibited LPA-stimulated RHOA and ERK pathway activation. Consistent with decreased signaling, CD97 depletion inhibited LPA-stimulated invasion. By contrast, CD97 depletion had a significantly smaller effect upon HGF-initiated signaling and invasion. Thus, CD97 action appears to be linked to LPA-initiated function. A complementary approach using reconstitution was performed in LNCaP cells, which do not normally express CD97 or LPAR1. In this case, CD97 increased LPA-initiated LPAR1-dependent invasion. These in vitro data were extended in vivo for PC3 cells, to demonstrate that CD97 depletion reduced metastatic colonization to the bone by more than half, suggesting an effect upon early tissue invasion and/or the establishment of micrometastases. Interestingly, in breast cancer, the LPA/LPAR pathway has been associated with bone metastases. In a xenograft model, LPAR signaling promoted both the establishment and subsequent expansion of osteolytic bone metastases (35).

We investigated the possibility that CD97-LPAR heterodimerization could mechanistically explain the positive effect of CD97 expression on LPA-initiated signaling. Using both ectopic expression and shRNA-mediated depletion, it was possible to demonstrate physical complex formation between epitope-tagged LPAR1 and either tagged or endogenously-expressed CD97. It is possible that there exist additional interactions between CD97 and other GPCRs. However, one measure of specificity for the LPAR-CD97 interaction was indicated by the lack of physical and functional interaction between CD97 and CXCR4, a GPCR that has been suggested to play a role in prostate cancer invasion(36). Immunohistological analysis of clinical prostate cancer samples revealed that LPAR1 is expressed in normal prostate and in about 80% of adenocarcinomas, with relatively increased levels compared to normal epithelium. There was a significant association of CD97 and LPAR1 expression in adenocarcinomas, confirming the potential for these receptors to synergize in prostate cancers. The role of the LPA-LPAR axis in tumorigenesis and metastasis has been well established (15). Thus, the data presented here provide a mechanistic rationale for induced CD97 expression in prostate carcinomas. Further analysis to test for the generality of the LPAR-CD97 association across tissue types will be of interest.

We describe the positive regulation by CD97 of ligand-dependent LPAR1 signaling. We have found no indication for ligand-dependent CD97 function in the context investigated here. For serum stimulated invasion of prostate cancer cells, there were no effects of blocking antibodies directed to previously identified CD97 cell surface ligands including integrins α5β1 and αvβ3 as well as CD55. Of course, we cannot exclude the possibility that other unidentified CD97 ligands are required. Thus, preliminarily, CD97 and LPAR1 heterodimerization appears to exemplify ligand independent (CD97) regulation of ligand-dependent (LPAR) GPCR function. Several mechanisms have been identified for other heterodimerized GPCR's that account for positive regulation by a ligand-independent

partner (37). Since both CD97 and LPAR1 couple to $G\alpha_{12/13}$, one potential mechanism of synergy is the reinforcement or amplification of RHO-dependent signaling (15).

The data presented here have practical implications. LPA receptors are considered promising therapeutic targets for cancer treatment, and drugs that inhibit the LPA-LPAR axis are being developed (38). Increased expression of CD97 has been observed in a number of carcinomas and induced expression of the closely-related receptor, EMR2, has been described in breast cancer (39). The presence of CD97 (and possibly EMR2) should be included in the analysis of efficacy for LPAR directed treatment. In addition, modulating CD97 expression with therapeutic antibodies or small molecule inhibitors directed to the 7TM pocket are potential approaches to modifying LPAR responses.

Supplementary Material

Refer to Web version on PubMed Central for supplementary material.

Acknowledgements

We acknowledge the support of the Intramural Research Program, Center for Cancer Research, National Cancer Institute. We thank our many generous colleagues for sharing cell lines and reagents. We acknowledge Barbara J Taylor and Subhadra Banerjee of the CCR FACS Core Facility and Theresa Davies-Hill for her excellent technical assistance.

References

1. Gray JX, Haino M, Roth MJ, Maguire JE, Jensen PN, Yarme A, et al. CD97 is a processed, seven-transmembrane, heterodimeric receptor associated with inflammation. J Immunol. 1996;157:5438–47. [PubMed: 8955192]
2. Yona S, Lin HH, Siu WO, Gordon S, Stacey M. Adhesion-GPCRs: emerging roles for novel receptors. Trends Biochem Sci. 2008;33:491–500. [PubMed: 18789697]
3. Aust G, Steinert M, Schutz A, Boltze C, Wahlbuhl M, Hamann J, et al. CD97, but not its closely related EGF-TM7 family member EMR2, is expressed on gastric, pancreatic, and esophageal carcinomas. Am J Clin Pathol. 2002;118:699–707. [PubMed: 12428789]
4. Steinert M, Wobus M, Boltze C, Schutz A, Wahlbuhl M, Hamann J, et al. Expression and regulation of CD97 in colorectal carcinoma cell lines and tumor tissues. Am J Pathol. 2002;161:1657–67. [PubMed: 12414513]
5. Mustafa T, Eckert A, Klonisch T, Kehlen A, Maurer P, Klintschar M, et al. Expression of the epidermal growth factor seven-transmembrane member CD97 correlates with grading and staging in human oral squamous cell carcinomas. Cancer Epidemiol Biomarkers Prev. 2005;14:108–19. [PubMed: 15668483]
6. Loberg RD, Wojno KJ, Day LL, Pienta KJ. Analysis of membrane-bound complement regulatory proteins in prostate cancer. Urology. 2005;66:1321–6. [PubMed: 16360477]
7. Lagerstrom MC, Schioth HB. Structural diversity of G protein-coupled receptors and significance for drug discovery. Nat Rev Drug Discov. 2008;7:339–57. [PubMed: 18382464]
8. Iguchi T, Sakata K, Yoshizaki K, Tago K, Mizuno N, Itoh H. Orphan G protein-coupled receptor GPR56 regulates neural progenitor cell migration via a G alpha 12/13 and Rho pathway. J Biol Chem. 2008;283:14469–78. [PubMed: 18378689]
9. Xu L, Begum S, Hearn JD, Hynes RO. GPR56, an atypical G protein-coupled receptor, binds tissue transglutaminase, TG2, and inhibits melanoma tumor growth and metastasis. Proc Natl Acad Sci U S A. 2006;103:9023–8. [PubMed: 16757564]

10. Park D, Tosello-Trampont AC, Elliott MR, Lu M, Haney LB, Ma Z, et al. BAI1 is an engulfment receptor for apoptotic cells upstream of the ELMO/Dock180/Rac module. Nature. 2007;450:430–4. [PubMed: 17960134]
11. Silva JP, Lelianova V, Hopkins C, Volynski KE, Ushkaryov Y. Functional cross-interaction of the fragments produced by the cleavage of distinct adhesion G-protein-coupled receptors. J Biol Chem. 2009;284:6495–506. [PubMed: 19124473]
12. Wang T, Ward Y, Tian L, Lake R, Guedez L, Stetler-Stevenson WG, et al. CD97, an adhesion receptor on inflammatory cells, stimulates angiogenesis through binding integrin counterreceptors on endothelial cells. Blood. 2005;105:2836–44. [PubMed: 15576472]
13. Hamann J, Vogel B, van Schijndel GM, van Lier RA. The seven-span transmembrane receptor CD97 has a cellular ligand (CD55, DAF). J Exp Med. 1996;184:1185–9. [PubMed: 9064337]
14. Kwakkenbos MJ, Pouwels W, Matmati M, Stacey M, Lin HH, Gordon S, et al. Expression of the largest CD97 and EMR2 isoforms on leukocytes facilitates a specific interaction with chondroitin sulfate on B cells. J Leukoc Biol. 2005;77:112–9. [PubMed: 15498814]
15. Lin ME, Herr DR, Chun J. Lysophosphatidic acid (LPA) receptors: signaling properties and disease relevance. Prostaglandins Other Lipid Mediat. 2010;91:130–8. [PubMed: 20331961]
16. Stortelers C, Kerkhoven R, Moolenaar WH. Multiple actions of lysophosphatidic acid on fibroblasts revealed by transcriptional profiling. BMC Genomics. 2008;9:387. [PubMed: 18702810]
17. Xu Y, Gaudette DC, Boynton JD, Frankel A, Fang XJ, Sharma A, et al. Characterization of an ovarian cancer activating factor in ascites from ovarian cancer patients. Clin Cancer Res. 1995;1:1223–32. [PubMed: 9815916]
18. Guo R, Kasbohm EA, Arora P, Sample CJ, Baban B, Sud N, et al. Expression and function of lysophosphatidic acid LPA1 receptor in prostate cancer cells. Endocrinology. 2006;147:4883–92. [PubMed: 16809448]
19. Kitayama J, Shida D, Sako A, Ishikawa M, Hama K, Aoki J, et al. Over-expression of lysophosphatidic acid receptor-2 in human invasive ductal carcinoma. Breast Cancer Res. 2004;6:R640–6. [PubMed: 15535846]
20. Liu S, Umezu-Goto M, Murph M, Lu Y, Liu W, Zhang F, et al. Expression of autotaxin and lysophosphatidic acid receptors increases mammary tumorigenesis, invasion, and metastases. Cancer Cell. 2009;15:539–50. [PubMed: 19477432]
21. Yin J, Pollock C, Tracy K, Chock M, Martin P, Oberst M, et al. Activation of the RalGEF/Ral pathway promotes prostate cancer metastasis to bone. Mol Cell Biol. 2007;27:7538–50. [PubMed: 17709381]
22. Polgar O, Ierano C, Tamaki A, Stanley B, Ward Y, Xia D, et al. Mutational analysis of threonine 402 adjacent to the GXXXG dimerization motif in transmembrane segment 1 of ABCG2. Biochemistry.49:2235–45.
23. Yang GC, Wan LS, Papellas J, Waisman J. Compact cell blocks. Use for body fluids, fine needle aspirations and endometrial brush biopsies. Acta Cytol. 1998;42:703–6. [PubMed: 9622691]
24. Ward Y, Spinelli B, Quon MJ, Chen H, Ikeda SR, Kelly K. Phosphorylation of critical serine residues in Gem separates cytoskeletal reorganization from down-regulation of calcium channel activity. Mol Cell Biol. 2004;24:651–61. [PubMed: 14701738]
25. Ward Y, Wang W, Woodhouse E, Linnoila I, Liotta L, Kelly K. Signal pathways which promote invasion and metastasis: critical and distinct contributions of extracellular signal-regulated kinase and Ral-specific guanine exchange factor pathways. Mol Cell Biol. 2001;21:5958–69. [PubMed: 11486034]
26. Smit MJ, Vischer HF, Bakker RA, Jongejan A, Timmerman H, Pardo L, et al. Pharmacogenomic and structural analysis of constitutive g protein-coupled receptor activity. Annu Rev Pharmacol Toxicol. 2007;47:53–87. [PubMed: 17029567]
27. Fromm C, Coso OA, Montaner S, Xu N, Gutkind JS. The small GTP-binding protein Rho links G protein-coupled receptors and Galpha12 to the serum response element and to cellular transformation. Proc Natl Acad Sci U S A. 1997;94:10098–103. [PubMed: 9294169]

28. Hao F, Tan M, Xu X, Han J, Miller DD, Tigyi G, et al. Lysophosphatidic acid induces prostate cancer PC3 cell migration via activation of LPA(1), p42 and p38alpha. Biochim Biophys Acta. 2007;1771:883–92. [PubMed: 17531530]
29. Ahmed T, Shea K, Masters JR, Jones GE, Wells CM. A PAK4-LIMK1 pathway drives prostate cancer cell migration downstream of HGF. Cell Signal. 2008;20:1320–8. [PubMed: 18424072]
30. Gmyrek GA, Walburg M, Webb CP, Yu HM, You X, Vaughan ED, et al. Normal and malignant prostate epithelial cells differ in their response to hepatocyte growth factor/scatter factor. Am J Pathol. 2001;159:579–90. [PubMed: 11485916]
31. Wells CM, Ahmed T, Masters JR, Jones GE. Rho family GTPases are activated during HGF-stimulated prostate cancer-cell scattering. Cell Motil Cytoskeleton. 2005;62:180–94. [PubMed: 16211585]
32. Fischer OM, Giordano S, Comoglio PM, Ullrich A. Reactive oxygen species mediate Met receptor transactivation by G protein-coupled receptors and the epidermal growth factor receptor in human carcinoma cells. J Biol Chem. 2004;279:28970–8. [PubMed: 15123705]
33. Shida D, Kitayama J, Yamaguchi H, Hama K, Aoki J, Arai H, et al. Dual mode regulation of migration by lysophosphatidic acid in human gastric cancer cells. Exp Cell Res. 2004;301:168–78. [PubMed: 15530853]
34. Thymiakou E, Episkopou V. Detection of signaling effector-complexes downstream of bmp4 using PLA, a proximity ligation assay. J Vis Exp. 2011.
35. Boucharaba A, Serre CM, Gres S, Saulnier-Blache JS, Bordet JC, Guglielmi J, et al. Platelet-derived lysophosphatidic acid supports the progression of osteolytic bone metastases in breast cancer. J Clin Invest. 2004;114:1714–25. [PubMed: 15599396]
36. Singh S, Singh UP, Grizzle WE, Lillard JW Jr. CXCL12-CXCR4 interactions modulate prostate cancer cell migration, metalloproteinase expression and invasion. Lab Invest. 2004;84:1666–76. [PubMed: 15467730]
37. Levoye A, Dam J, Ayoub MA, Guillaume JL, Jockers R. Do orphan G-protein-coupled receptors have ligand-independent functions? New insights from receptor heterodimers. EMBO Rep. 2006;7:1094–8. [PubMed: 17077864]
38. Gupte R, Patil R, Liu J, Wang Y, Lee SC, Fujiwara Y, et al. Benzyl and naphthalene methylphosphonic acid inhibitors of autotaxin with anti-invasive and anti-metastatic activity. ChemMedChem. 2011;6:922–35. [PubMed: 21465666]
39. Davies JQ, Lin HH, Stacey M, Yona S, Chang GW, Gordon S, et al. Leukocyte adhesion-GPCR EMR2 is aberrantly expressed in human breast carcinomas and is associated with patient survival. Oncol Rep. 2011;25:619–27. [PubMed: 21174063]

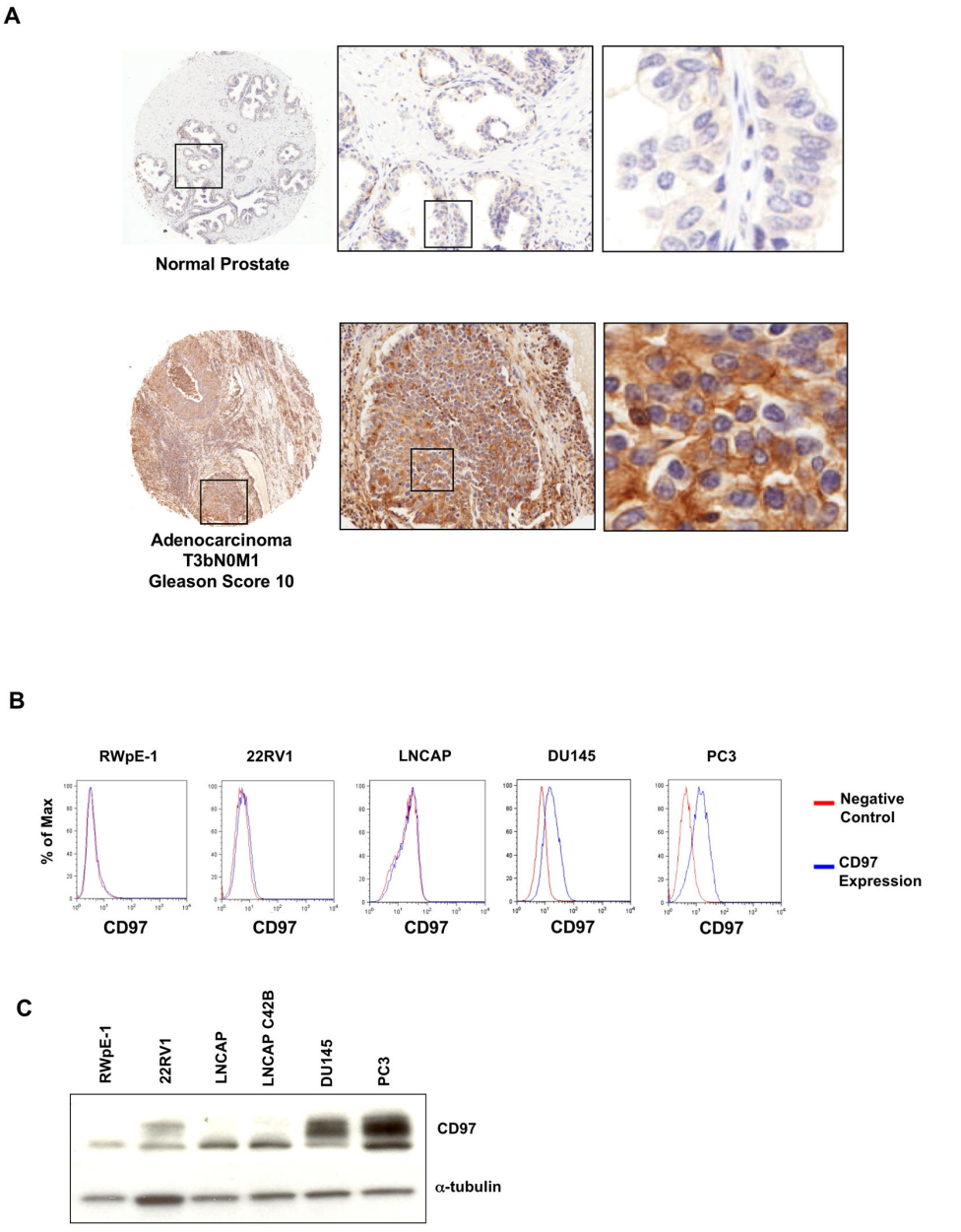

Figure 1.

CD97 is expressed in human prostate cancer and in cell lines derived from prostate carcinoma (**A**) CD97 expression in human prostate adenocarcinoma and in matched normal adjacent tissue in a prostate cancer tissue array (US Biomax, Inc). The tissue microarray was stained for CD97 using a rabbit polyclonal antibody.(**B**) Surface expression of CD97 as determined by Facs analysis in immortalized normal prostate epithelial cells and prostate cancer cell lines. (**C**) Western blot depicting total CD97 expression in the cell lines shown in (B).

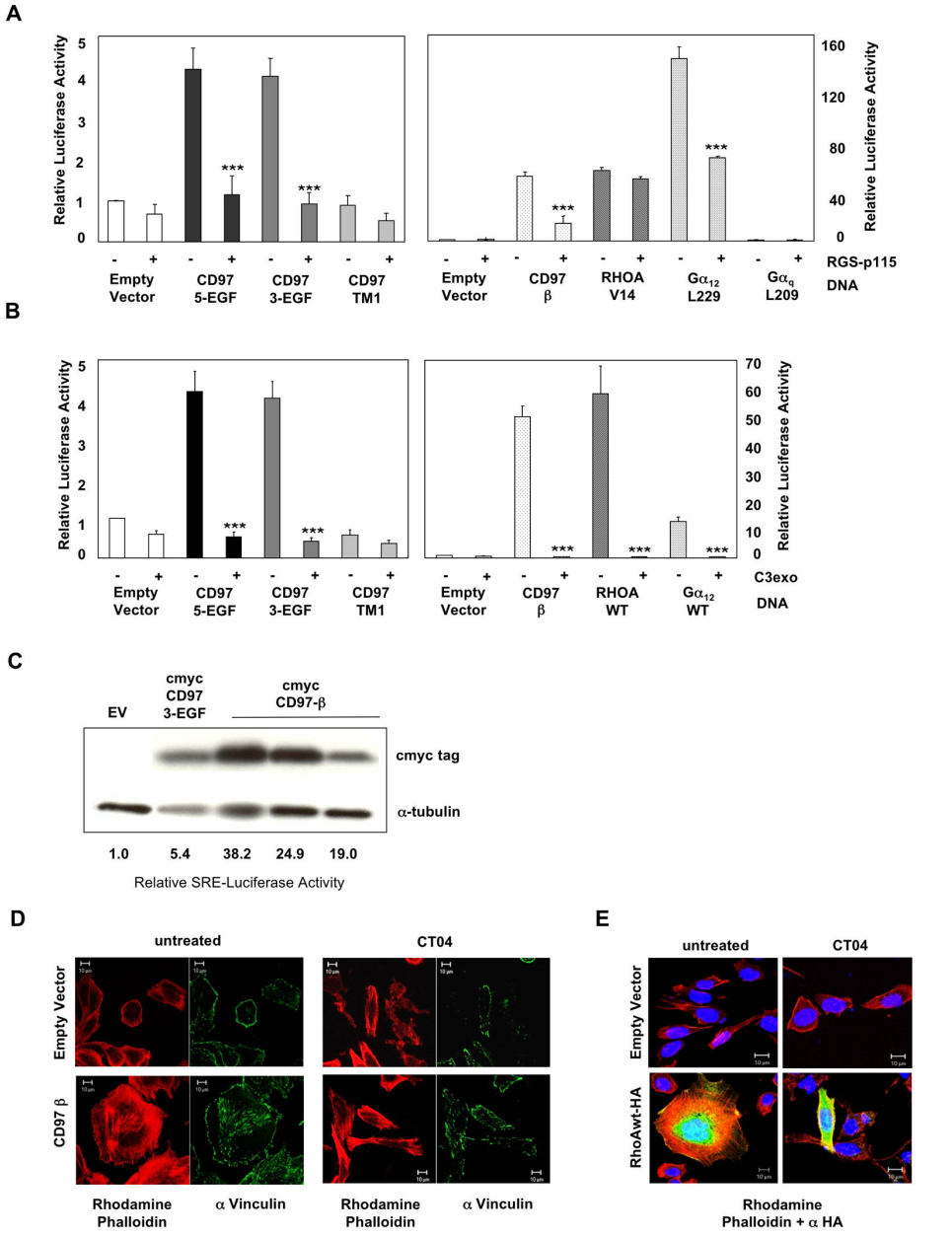

Figure 2.

CD97 induces $G\alpha_{12/13}$-mediated RHOA-dependent signaling (**A**) COS 7 cells were transfected with the SRE-luciferase reporter construct and the indicated expression plasmids. Cells were assayed with or without cotransfection of the RGS domain of p115GEF. (**B**) The SRE-luciferase assay in (A) was performed in the presence or absence of an expression construct for C3 exoenzyme to specifically inhibit RHO activity. Reporter activities represent the means ±SD from 4 independent experiments.***denotes P<0.0001 by unpaired *t* test. (**C**) Relative SRE-luciferase activity was determined for measured levels of myc epitope-tagged CD97–3EGF and myc epitope-tagged CD97-β protein expression. (**D**) CHO cell clones expressing empty vector or CD97-β were stained for actin (red) and vinculin (green). Cells were either left untreated or treated with 4μg/ml CT04 for 2 hours prior to

fixation. Representative confocal images are shown. (**E**) CHO cells transiently transfected with HA-tagged wild type RHOA were incubated with or without 4μg/ml CT04 and stained for actin (red) and HA-RHOA (green). DAPI stain was used to visualize cell nuclei. Representative merged confocal images are shown.

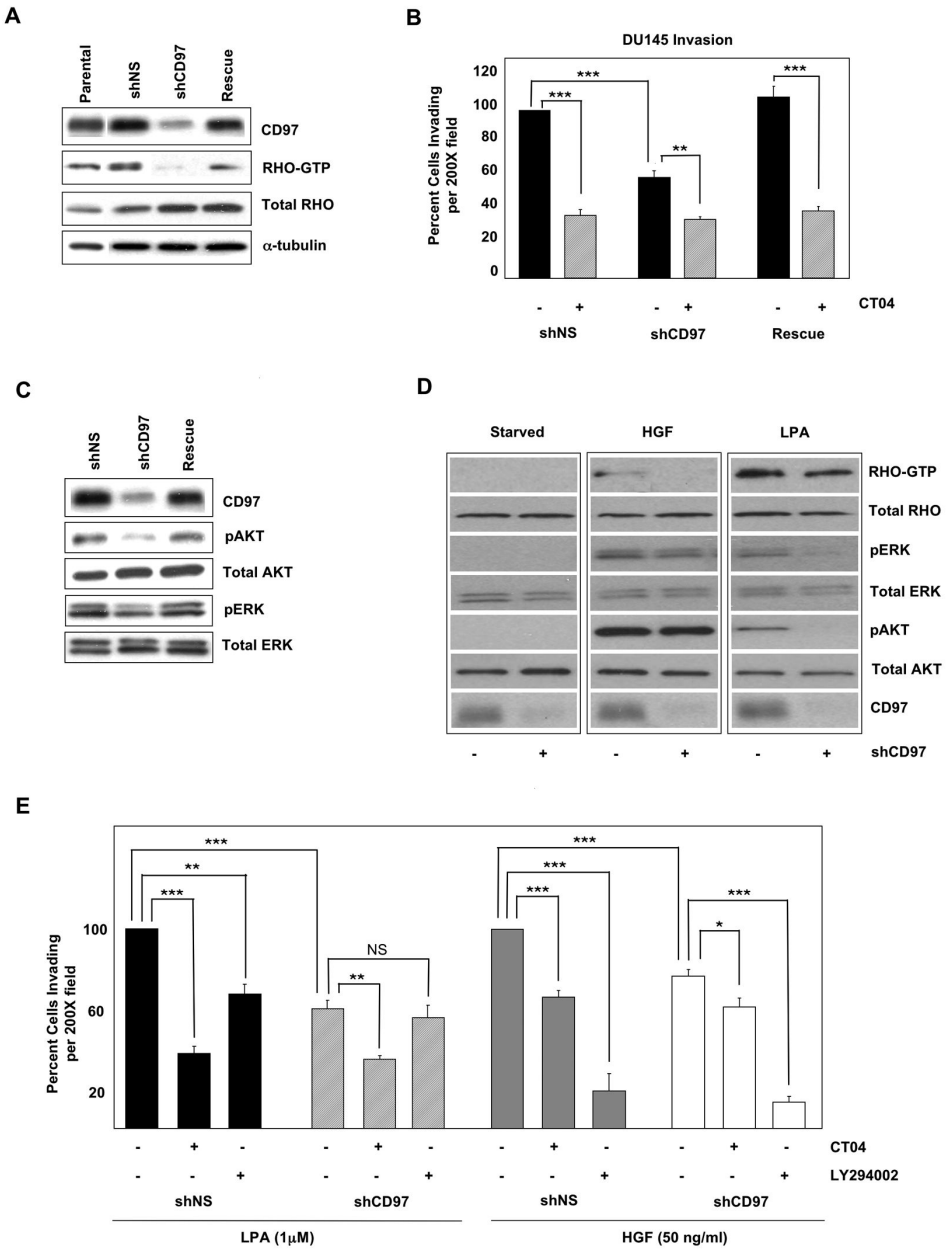

Figure 3.

Depletion of CD97 in DU145 cells leads to decreased invasion in vitro and downregulation of RHO-GTP, phospho-ERK, and phospho-AKT. **(A)** Western blot showing CD97 expression and RHO-GTP levels in DU145 cells depleted for CD97 (shCD97), infected with non-silencing shRNA (shNS), or rescued by nontargetable CD97 expression (rescue). (**B**) Invasion of the cells described in (A) through matrigel toward the chemoattractant 10% FCS. Invasive cells in five microscopic fields (200X) were counted. **(C)** Western blot analysis showing phosphorylated ERK and AKT in cells growing in serum. (**D**) HGF and LPA stimulated RHO, ERK, and AKT activation in control and CD97-depleted DU145 cells were assayed by western blot. **(E)** Cellular invasion by either control or CD97-depleted DU145 cells to LPA (1μM) or HGF (50 ng/ml) with or without CT04 (1μg/ml) or LY294002 (15μM)

pretreatment. All results shown are representative of at least four independent experiments. Error bars represent ±SEM. ***P<0.0001, **P<0.001, *P<0.01, NS = non-significant difference at a 95% confidence interval.

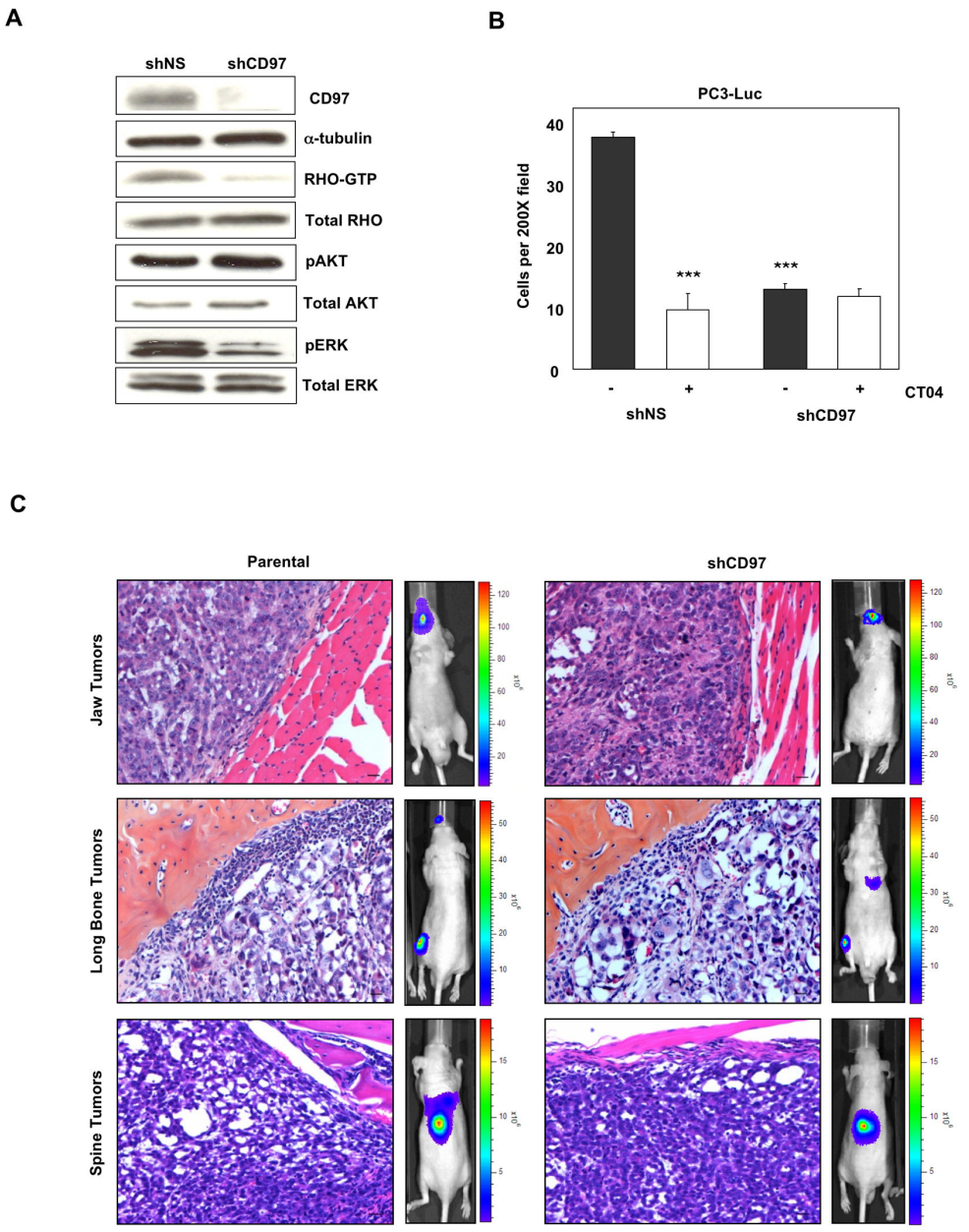

Figure 4.

Depletion of CD97 in PC3 cells results in downregulation of RHO and ERK, and reduced invasion in vitro. **(A)** PC3 cells depleted for CD97 (shCD97) or expressing a non-silencing (NS) shRNA control were assayed for the indicated proteins by western blot analysis. Binding to GST-Rhotekin was used to pull down GTP-bound RHOA. (**B**) Invasion of PC3 cells to LPA with or without (1μg/ml) CT04 pretreatment. Invasive cells in five microscopic fields (200X) were counted. All results shown are representative of at least four independent experiments. Error bars represent ±SEM. ***P<0.0001 (**C**) Representative bioluminescence images from jaw, long bone or spine metastasis are shown next to corresponding histological sections stained with H&E and Orange G.

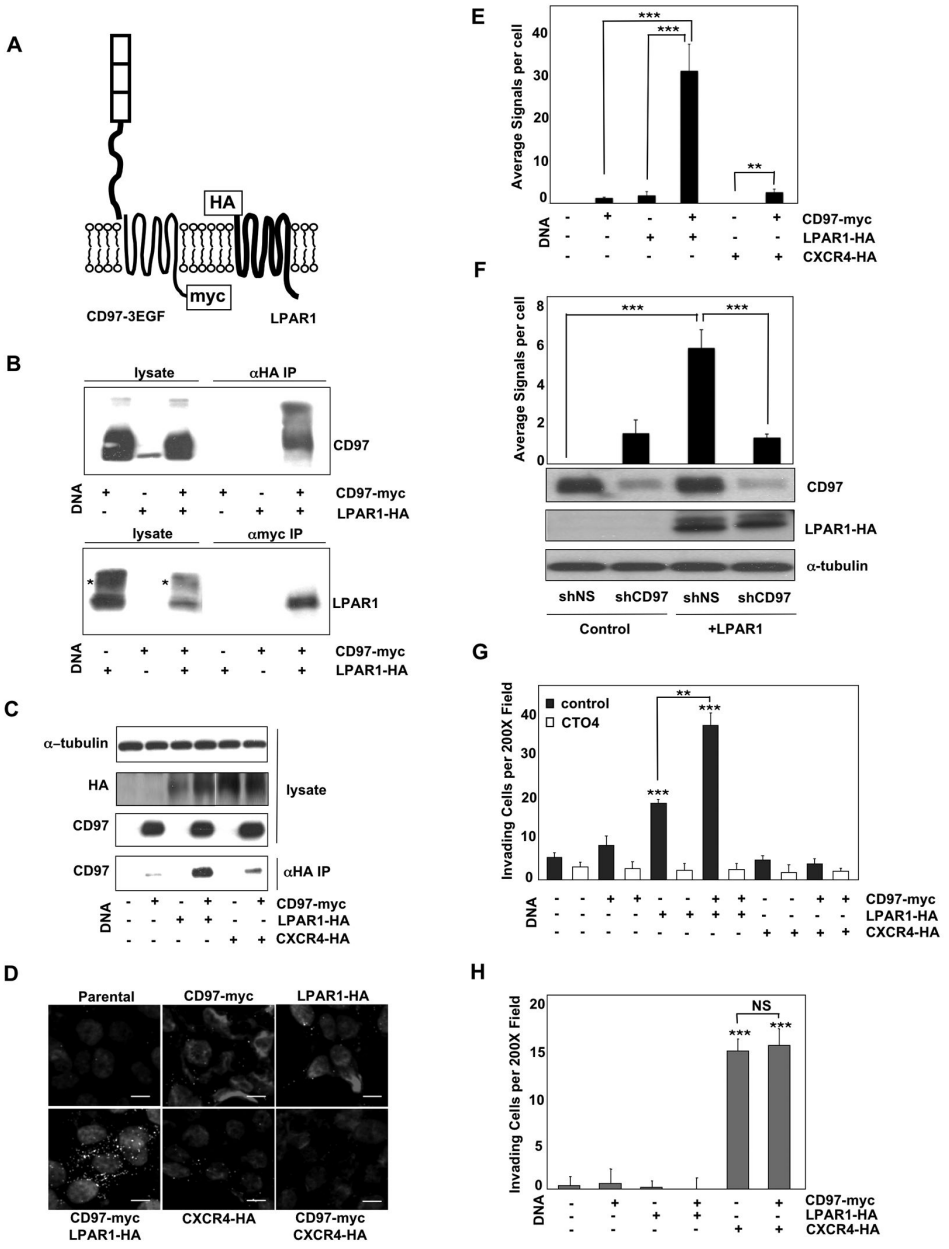

Figure 5.

CD97 interacts with LPA receptor to potentiate LPA initiated RHO-dependent invasion in vitro. (**A**) Schematic of myc-tagged CD97–3EGF and HA-tagged LPAR1. (**B**) Coimmunoprecipitation of LPAR1 and CD97 in CHO cells transiently transfected with CD97 and/or LPAR1. The antibodies used for immunoprecipitation and western blotting are indicated on the top and side of each panel respectively. * indicates a background band. (**C**) Coimmunoprecipitation of CD97 with LPAR1 or CXCR4 in permanently transduced LNCaP cells. Antibodies used for western blotting are indicated on the left. (**D**) Stable LNCaP cell lines expressing the indicated proteins were subjected to in situ proximity ligation assays (PLA). The detected heterodimers are depicted by the red fluorescent dots and nuclei are stained blue with DAPI. Representative microscopic fields are shown and scale bars

represent 10μM. (**E**) Quantification of PLA results was carried out using the Duolink Image Tool software. (**F**) In situ PLA was performed for parental and CD97-depleted DU145 cells permanently transduced with empty vector or LPAR1. The relative expression levels of CD97 and LPAR1 are shown. (**G**) LNCaP cells permanently expressing the indicated proteins were assayed for their invasive activity to LPA. Invading cells in five microscopic fields (200X) were counted. To demonstrate that invasion was RHO-dependent, cells were treated with 1μg/ml CT04 before being loaded into the transwell chamber. (**H**) Human SDF-1α (50ng/ml) was substituted for LPA in the invasion assay described above. Results for (E-H) are representative of four independent experiments. Error bars represent ±SEM. ***P<0.0001, **P<0.001, NS = non-significant difference at a 95% confidence interval.

Table 1

Scoring of CD97 and LPAR1 expression in a prostate tissue array

Scoring	LPAR1					CD97			
	−	+/−	+	++		−	+/−	+	++
Normal N=15	13.3%	66.7%	20.0%	0		100%	0	0	0
Adenocarcinoma Gleason 6–7 N=28	28.6%	35.7%	35.7%	0		32.1%	3.5%	50.0%	14.4%
Adenocarcinoma Gleason 8–10 N=40	15.0%	27.5%	37.5%	20.0%		47.5%	5.0%	40.0%	7.5%
Total Adenocarcinoma N=68	20.6%	30.9%	36.7%	11.8%		41.2%	4.4%	44.1%	10.3%

Staining of CD97 was scored based on the number of cells expressing CD97. The intensity of staining was uniform and localized to cell membranes, cytoplasm, and nuclei. Representative CD97 staining in the prostate tissue array is depicted in Figure 1.

++ CD97 expressed in most or all cells (80–100%), + CD97 expressed in a significant number of cells (50–80%), +/− CD97 expressed in a minority of the cells (<50%), - CD97 absent. LPAR1 staining was scored based on intensity which varied between cores. When staining was positive, most cells expressed LPAR1 (80–100%). ++ intense staining, + moderate staining, +/− weak staining, - no staining. Representative degrees of LPAR1 staining used to score the prostate tissue array are shown in Supplementary Figure 4. In adenocarcinomas there was a significant correlation between the presence of CD97 and LPAR1 expression ($P \leq 0.01$, Fisher's Exact Test)

Table 2

Relative metastatic potential of control PC3 cells and CD97 depleted PC3 cells

PC3 Luciferase Cell Line	Mice with Metastasis	Total Metastases	Average Mets per Mouse	Total Jaw Metastases	Total Long Bone Metastases	Total Spine Metastases
Parental N=15	93.3%	31	2.07 (±0.33)	20	8	3
shCD97 N=22	54.5%	17	0.77 (±0.17)	12	4	1

PC3-luc (parental) or PC3-luc shRNA expressing cells (shCD97) were injected into the left ventricle of athymic male mice. Tumors were scored as positive if a bioluminescent signal in the identical location was detected for at least three consecutive weeks. Shown are percent mice with metastasis, absolute numbers of tumors, and average number of tumors per mouse ±SEM; P=0.0006 by unpaired t test. Also displayed is the organ distribution of tumors. Metastases in a subset of mice were verified with necropsies and histological analyses. The results shown are the combined results from two independent experiments. Experiments were terminated at week 7 at which time >90% of mice were euthanized due to morbidity.